

Predicting Stellar Angular Diameters from V , I_C , H , K Photometry

Arthur D. Adams,^{1*} Tabettha S. Boyajian,^{1,2} Kaspar von Braun³

¹Department of Astronomy, Yale University, 52 Hillhouse Avenue, New Haven, CT 06511, USA

²Department of Physics and Astronomy, Louisiana State University, Nicholson Hall, Tower Drive, Baton Rouge, LA 70803, USA

³Lowell Observatory, 1400 W. Mars Hill Road, Flagstaff, AZ 86001, USA

Accepted XXX. Received YYY; in original form ZZZ

ABSTRACT

Determining the physical properties of microlensing events depends on having accurate angular sizes of the source star. Using long-baseline optical interferometry we are able to measure the angular sizes of nearby stars with uncertainties $\leq 2\%$. We present empirically derived relations of angular diameters that are calibrated using both a sample of dwarfs/subgiants and a sample of giant stars. These relations are functions of five color indices in the visible and near-infrared, and have uncertainties of 1.8–6.5% depending on the color used. We find that a combined sample of both main-sequence and evolved stars of A–K spectral types is well fit by a single relation for each color considered. We find that in the colors considered, metallicity does not play a statistically significant role in predicting stellar size, leading to a means of predicting observed sizes of stars from color alone.

Key words: planetary systems — stars: early-type — stars: fundamental parameters — stars: general — stars: late-type

1 INTRODUCTION

Precise stellar radius measurements are important for many subfields of astronomy, especially for exoplanet characterization. While precise radii are most readily applicable to transiting exoplanet characterization, they also correspond directly to stellar angular diameters. One notable application for such angular diameters is in constraining the physical properties of microlensing events, for example in distinguishing cases of self-lensing from those of MACHO lensing (Calchi Novati et al. 2010; Fukui et al. 2015).

Microlensing systems are often far too distant for direct measurements of the stellar angular size, prompting empirical means to determine stellar sizes from photometry alone.

The surface brightness of a star for a given magnitude is defined in terms of the magnitude and angular diameter (Wesselink 1969; Barnes & Evans 1976; Di Benedetto 2005):

$$S_V = V_0 + 5 \log \theta \quad (1)$$

where V_0 is an intrinsic magnitude set such that $S_V = V_0$ when the angular diameter $\theta = 1$ mas.

Wesselink (1969) demonstrates a strong empirical correlation between surface brightness and $(B - V)$ color; a more general correlation between surface brightnesses and color

indices has been shown in Barnes & Evans (1976). Therefore we expect to be able to construct relations between stellar angular size, color, and an apparent magnitude from the given color. Barnes & Evans (1976) further demonstrate that surface brightness is independent of stellar luminosity class, which implies that such an angular size-color-magnitude relation should hold regardless of whether stars have evolved off the main sequence. Di Benedetto (2005) proposed, through comparison of their empirical relations for both dwarf and giant stars, that there was enough overlap in the then available data to motivate a combined fit across evolutionary stages.

One photometric magnitude of each color is used as a baseline for developing a *zero-magnitude diameter*, the angular diameter each star would appear to have if its apparent magnitude were zero in a selected band:

$$\log \theta_{Q=0} = \log \theta_{LD} + 0.2Q \quad (2)$$

where θ_{LD} is the angular diameter after correction for limb-darkening and Q is the magnitude in a given band. We construct our relations as polynomials in color. For a given color $(P - Q)$

$$\log \theta_{Q=0} = \sum_{n=0}^N c_n (P - Q)^n \quad (3)$$

where N is an arbitrary order, taken to be the greatest statistically significant order when fitting the data. Determina-

* E-mail: arthur.adams@yale.edu

tion of angular sizes from observed colors is insensitive to wavelength-dependent extinction for the precisions attainable through this analysis (Barnes & Evans 1976); therefore we neglect extinction correction.

The use of interferometry to measure the angular diameters of stars has played a major role in empirically constraining the radii of nearby stars. Our new relations benefit from recent precise angular diameter measurements of both main-sequence and evolved stars using optical interferometry. They extend the results of Boyajian et al. (2014) with new data and more precise relations for both main-sequence and evolved stars, constructed for a more limited range of spectral types.

Section 2 describes the criteria for data selection and sources of angular diameters and photometry, and the methodology for fitting the data is presented in Section 3. We analyze the results in Section 4, including a comparison with previous works (Section 4.1).

2 DATA

We compile a list of stars with both V , I_C , H , and/or K magnitudes and precise angular diameters in Tables 1–2. A total of 57 distinct main-sequence stars are selected among all relations, with effective temperatures of 3927–9553 K (spectral types A1–M0), a mean angular diameter uncertainty of 0.013 mas, and apparent V magnitudes of 0.03–7.70. The evolved sample contains 50 stars with effective temperatures of 3972–10330 K (spectral types A1–M0), a mean angular diameter uncertainty of 0.043 mas, and apparent V magnitudes of 1.16–6.18. The following subsections outline both the source information as well as selection and classification criteria.

2.1 Stellar Classification

We restrict included stars to an effective temperature range of $3900 < T < 10500$ K, which approximately captures spectral types A–K.

Evolved stars are selected not based on their listed spectral classes, but by a stellar radius cut of $6 < R_\star/R_\odot < 100$. This is done in an attempt to disambiguate the luminosity classes of stars which might have inconsistent classifications in the boundary between subgiants and giants.

Some stars in our sample are known to be in multiple star systems. The presence of additional stars can introduce an offset in flux and visibility of the target star. We adopt the selection precedent from Boyajian et al. (2008); we exclude any binary systems where a secondary star is both separated from the target by at most $5''$ and is within 3 magnitudes of the target in any bands used in the analysis.

2.2 Angular Diameters

All stars are required to have limb-darkened angular diameters with mean random errors $\leq 2\%$, and must have been observed on at least two separate occasions. The measurements come from a variety of sources, which are detailed in Boyajian et al. (2012b) and Boyajian et al. (2013) and listed for reference in Tables 1–2. Stars with inconsistent diameters (here defined as any 2 sources differing by at least 3

times the maximum uncertainty of any measurement) were excluded. We take the uncertainty-weighted means of the remaining measurements for our quoted angular diameters.

Angular diameter source instruments include the Palomar Testbed Interferometer, the Very Large Telescope Interferometer, the Sydney University Stellar Interferometer, the Narrabri Stellar Intensity Interferometer, the Mark III interferometer, the Navy Prototype Optical Interferometer, and especially the CHARA Array.

2.3 Magnitudes

2MASS photometry (Cutri et al. 2003) is saturated for most of the stars in our sample due to brightness. Therefore we rely on earlier photometric catalogs for reliable magnitudes. All magnitudes used are listed in Tables 1–2. For the I magnitudes we use Cousins I_C photometry converted from Johnson I_J sources (Mallama 2014), as well as magnitudes from Koen et al. (2010) for our reddest stars. We use Gezari et al. (1999) for H magnitudes, querying the catalog for all magnitude measurements centered at $1.65 \mu\text{m}$. Here, errors of 0.05 mag assumed as a conservative estimate. The K magnitudes are taken from a combination of Neugebauer & Leighton (1969), Kidger & Martín-Luis (2003), and Kimeswenger et al. (2004). Since the filter profiles for the magnitudes in these catalogs differ appreciably, we choose to convert all into the 2MASS system. Neugebauer & Leighton (1969) magnitudes are originally in the CIT system (Iyengar et al. 1982), and the Kimeswenger et al. (2004) are listed as DENIS K_5 magnitudes. Carpenter (2001) provide transformations from both the CIT and DENIS systems into the 2MASS system (with updated transformations available on the 2MASS website). For the Kidger & Martín-Luis (2003) magnitudes we first transform into an intermediate system, the Koornneef system (Koornneef 1983). Kidger & Martín-Luis (2003) compare their photometry to the system described in (Koornneef 1983) and find a constant offset in magnitude. From this we convert to 2MASS via the relation in Carpenter (2001). While significant color dependence exists for the DENIS and Koornneef transformations, the CIT transformation exhibits only a very weak color dependence. In light of this, and the lack of accompanying J magnitudes for the Neugebauer & Leighton (1969) K magnitudes, we choose to neglect the color term, incorporating the error from this omission into our final uncertainty propagation.

In order to calculate color indices, all stars must have at least one available magnitude in any of the I_C , H , and K bands. We exclude stars with inconsistent magnitudes: that is, magnitudes from different sources whose values disagree by at least triple the largest uncertainty of any one value. The listed uncertainties in the resulting colors are propagated from both the uncertainties from conversion as well as assumed 0.02 mag errors in the original Johnson V magnitudes (Mallama 2014).

3 FITTING PROCEDURE

We choose to construct relations for $V - I_C$, $V - H$, $V - K$, $I_C - H$, and $I_C - K$ (Figure 1). We start with a constant-only

Table 1. Selected Stellar Properties – Dwarfs

HIP	Sp. Type	θ_{LD} (mas)	V	I_C	H	K	θ_{LD} Ref.
3765	K2.5V	0.868 ± 0.004	5.740	4.780 ± 0.027	–	–	1
3821	F9V	1.623 ± 0.004	3.460	–	2.020 ± 0.050	1.821 ± 0.060	2
4151	F9V	0.865 ± 0.010	4.800	4.210 ± 0.027	3.560 ± 0.050	–	2
4436	A6V	0.708 ± 0.013	3.860	3.700 ± 0.027	3.370 ± 0.060	3.365 ± 0.071	3
5336	K1V Fe-2	0.972 ± 0.009	5.170	4.360 ± 0.027	–	–	4
7513	F9V	1.143 ± 0.010	4.100	3.500 ± 0.027	2.990 ± 0.050	2.841 ± 0.080	5, 6
7981	K1V	1.000 ± 0.004	5.240	4.360 ± 0.027	3.345 ± 0.050	–	7
8102	G8.5V	2.080 ± 0.030	3.490	2.630 ± 0.027	1.727 ± 0.050	1.631 ± 0.060	8
12114	K3V	1.030 ± 0.007	5.790	4.740 ± 0.027	3.542 ± 0.050	–	1
12777	F7V	1.103 ± 0.009	4.100	3.530 ± 0.027	3.070 ± 0.050	2.761 ± 0.090	2
16537	K2V (k)	2.126 ± 0.014	3.720	–	1.749 ± 0.050	1.601 ± 0.060	9
16852	F9IV-V	1.081 ± 0.014	4.290	3.640 ± 0.027	–	2.871 ± 0.100	2
19849	K0.5V	1.446 ± 0.022	4.430	3.530 ± 0.027	–	–	1, 10
22449	F6IV-V	1.419 ± 0.027	3.190	2.650 ± 0.027	2.148 ± 0.050	2.031 ± 0.060	11, 2
24813	G1V	0.981 ± 0.015	4.690	4.040 ± 0.027	3.330 ± 0.050	3.255 ± 0.045	2
27435	G2V	0.572 ± 0.009	5.970	–	4.499 ± 0.050	–	7
27913	G0V CH-0.3	1.051 ± 0.009	4.390	–	3.050 ± 0.050	2.971 ± 0.070	2
32349	A0mA1Va	5.959 ± 0.059	-1.440	-1.430 ± 0.027	-1.387 ± 0.050	–	12, 13, 14, 15, 16
32362	F5IV-V	1.401 ± 0.009	3.350	2.870 ± 0.027	–	2.111 ± 0.060	2
35350	A3V	0.835 ± 0.013	3.580	3.450 ± 0.027	–	–	2
36366	F1V	0.853 ± 0.014	4.160	3.780 ± 0.027	–	–	2
37279	F5IV-V	5.434 ± 0.050	0.400	-0.140 ± 0.027	-0.569 ± 0.050	-0.669 ± 0.051	13, 17, 18, 19
40843	F6V	0.706 ± 0.013	5.130	–	3.940 ± 0.050	–	7
43587	K0IV-V	0.711 ± 0.004	5.960	–	4.140 ± 0.050	–	20
45343	M0.0V	0.871 ± 0.015	7.640	–	4.253 ± 0.050	–	1
46733	F0V	1.133 ± 0.009	3.650	3.270 ± 0.027	–	2.711 ± 0.090	2
46853	F7V	1.632 ± 0.005	3.170	2.610 ± 0.027	2.025 ± 0.050	1.951 ± 0.070	2
47080	G8IV	0.821 ± 0.013	5.400	–	3.770 ± 0.050	–	2
51459	F8V	0.794 ± 0.014	4.820	4.240 ± 0.027	–	–	2
53910	A1IVspSr	1.149 ± 0.014	2.340	2.380 ± 0.027	–	2.361 ± 0.060	2
56997	G8V	0.910 ± 0.009	5.310	4.580 ± 0.027	–	–	2
57757	F8.5IV-V	1.431 ± 0.006	3.590	3.000 ± 0.027	2.345 ± 0.050	2.301 ± 0.060	2
57939	G8. V P	0.686 ± 0.006	6.420	5.570 ± 0.027	–	–	2, 21
64394	G0V	1.127 ± 0.011	4.230	3.620 ± 0.027	2.923 ± 0.050	2.851 ± 0.100	2
64924	G7V	1.073 ± 0.005	4.740	3.990 ± 0.027	–	–	22
65721	G5V	1.010 ± 0.020	4.970	4.190 ± 0.027	3.320 ± 0.050	–	5
66249	A2Van	0.852 ± 0.009	3.380	3.280 ± 0.027	3.050 ± 0.050	–	2
67927	G0IV	2.252 ± 0.036	2.680	2.080 ± 0.027	1.390 ± 0.050	1.291 ± 0.051	13, 18, 23, 24
71284	F4Vkf2mF1	0.841 ± 0.013	4.470	4.020 ± 0.027	3.516 ± 0.050	–	2
72567	F9IV-V	0.569 ± 0.011	5.860	–	4.530 ± 0.050	–	7
72659	G7V	1.196 ± 0.014	4.540	–	3.000 ± 0.050	2.651 ± 0.080	2
78459	G0V	0.735 ± 0.014	5.390	–	3.945 ± 0.050	3.901 ± 0.045	22
81300	K0V (k)	0.724 ± 0.011	5.770	–	3.910 ± 0.050	–	1
91262	A1V	3.280 ± 0.010	0.030	0.080 ± 0.027	0.004 ± 0.050	-0.079 ± 0.060	13, 16, 25, 26, 27
92043	F5.5IV-V	1.000 ± 0.006	4.190	3.660 ± 0.027	–	2.941 ± 0.090	2
93747	A1V	0.895 ± 0.017	2.990	2.990 ± 0.027	–	2.921 ± 0.080	2
96100	G9V	1.254 ± 0.012	4.670	3.850 ± 0.027	–	2.811 ± 0.080	4
96441	F3+ V	0.844 ± 0.009	4.490	4.020 ± 0.027	–	–	2, 6
96895	G1.5V	0.554 ± 0.011	5.990	5.440 ± 0.027	4.731 ± 0.050	4.569 ± 0.045	7
98505	K2V	0.385 ± 0.006	7.670	6.680 ± 0.008	–	–	28
102422	K0IV	2.650 ± 0.040	3.410	2.510 ± 0.027	–	1.201 ± 0.051	29
108870	K5V	1.881 ± 0.017	4.690	3.530 ± 0.027	–	–	10
112447	F6V	1.091 ± 0.008	4.200	3.590 ± 0.027	–	2.851 ± 0.080	2
113368	A4V	2.230 ± 0.020	1.170	1.090 ± 0.027	1.054 ± 0.050	0.981 ± 0.051	19
114570	F1V	0.648 ± 0.008	4.530	4.160 ± 0.027	–	–	3
114622	K3V	1.106 ± 0.007	5.570	4.470 ± 0.027	3.400 ± 0.050	–	1
116771	F7V	1.082 ± 0.009	4.130	3.520 ± 0.027	–	2.731 ± 0.080	2
120005	K7.0V	0.856 ± 0.016	7.700	–	4.253 ± 0.050	–	1

Note. — **Angular Diameter References:** (1) Boyajian et al. (2012b), (2) Boyajian et al. (2012a), (3) Maestro et al. (2013), (4) Boyajian et al. (2008), (5) Baines et al. (2008), (6) Ligi et al. (2012), (7) Boyajian et al. (2013), (8) Di Folco et al. (2004), (9) di Folco et al. (2007), (10) Demory et al. (2009), (11) van Belle et al. (2009), (12) Davis & Tango (1986), (13) Mozurkewich et al. (2003), (14) Kervella et al. (2003), (15) Davis et al. (2011), (16) Hanbury Brown et al. (1974), (17) Chiavassa et al. (2012), (18) Nordgren et al. (2001), (19) Kervella et al. (2004a), (20) von Braun et al. (2011), (21) Crepp et al. (2012), (22) von Braun et al. (2014), (23) van Leeuwen (2007), (24) Thévenin et al. (2005), (25) Ciardi et al. (2001), (26) Aufdenberg et al. (2006), (27) Monnier et al. (2012), (28) Boyajian et al. (2015), (29) Nordgren et al. (1999). **Color Magnitude References:** Neugebauer & Leighton (1969), Gezari et al. (1999), Carpenter (2001), Kidger & Martín-Luis (2003), Kimeswenger et al. (2004), Koen et al. (2010), and Mallama (2014); see Section 2 for more details.

Table 2. Selected Stellar Properties – Giants

HIP	Sp. Type	θ_{LD} (mas)	V	I_C	H	K	θ_{LD} Ref.
3092	K3III	4.168 ± 0.047	3.270	2.040 ± 0.027	0.551 ± 0.050	0.421 ± 0.051	1, 2
7607	K3- III CN0.5	3.760 ± 0.070	3.590	2.310 ± 0.027	–	0.771 ± 0.041	3
7884	K2/3 III	2.810 ± 0.030	4.450	3.050 ± 0.027	1.409 ± 0.050	1.241 ± 0.031	3
9884	K1IIIb	6.847 ± 0.071	2.010	0.860 ± 0.027	-0.558 ± 0.050	-0.649 ± 0.051	1, 2, 3, 4
13328	K5.5III	4.060 ± 0.040	4.560	2.820 ± 0.027	–	0.721 ± 0.051	1
20205	G9.5IIIab CN0.5	2.520 ± 0.030	3.650	–	1.500 ± 0.050	1.481 ± 0.041	5
20455	G9.5III CN0.5	2.302 ± 0.040	3.770	–	–	1.581 ± 0.051	1, 2, 5
20885	G9III Fe-0.5	2.310 ± 0.040	3.840	–	–	1.621 ± 0.060	5
20889	G9.5III CN0.5	2.572 ± 0.046	3.530	–	–	1.291 ± 0.051	1, 2, 5, 6
21421	K5III	20.297 ± 0.384	0.870	–	-2.653 ± 0.050	–	1, 4, 7, 8
22453	K3+ III	2.727 ± 0.013	4.890	–	–	1.441 ± 0.041	9
37826	G9III	8.177 ± 0.130	1.160	0.160 ± 0.027	-1.003 ± 0.050	-1.139 ± 0.051	1, 10, 11, 2, 4
42527	K1+ III	2.225 ± 0.020	4.590	3.420 ± 0.027	1.941 ± 0.009	1.901 ± 0.070	12
45860	K6III	8.025 ± 0.142	3.140	1.460 ± 0.027	-0.475 ± 0.050	-0.699 ± 0.031	1, 11, 13, 2
46390	K3IIIa	9.700 ± 0.100	1.990	0.550 ± 0.027	-1.074 ± 0.050	-1.379 ± 0.060	1
49637	K3.5IIIb Fe-1:	3.330 ± 0.040	4.390	2.890 ± 0.027	1.190 ± 0.050	1.011 ± 0.070	3
53229	K0+ III-IV	2.540 ± 0.030	3.790	2.770 ± 0.027	–	1.351 ± 0.041	3
54539	K1III	4.107 ± 0.053	3.000	1.920 ± 0.027	0.539 ± 0.010	0.371 ± 0.041	1, 2
55219	K0IV	4.745 ± 0.060	3.490	2.110 ± 0.027	0.415 ± 0.010	0.251 ± 0.041	1, 2
56343	G7III	2.386 ± 0.021	3.540	2.620 ± 0.027	1.577 ± 0.050	1.491 ± 0.060	14
57399	K0.5IIIb:	3.230 ± 0.020	3.690	2.580 ± 0.027	1.020 ± 0.050	0.901 ± 0.031	3
57477	K2.5IIIb CN1	1.606 ± 0.006	5.270	–	–	2.531 ± 0.060	12
59746	K2III	1.498 ± 0.028	5.720	–	–	2.921 ± 0.080	12
60202	K0III	1.651 ± 0.016	4.720	3.720 ± 0.027	–	2.321 ± 0.051	15
63608	G8III	3.254 ± 0.037	2.850	1.970 ± 0.027	0.770 ± 0.050	0.731 ± 0.051	1, 2, 3
67459	K5.5III	4.720 ± 0.050	4.050	2.440 ± 0.027	–	0.391 ± 0.041	3
68594	G8:III: Fe-5	0.948 ± 0.012	6.180	–	3.775 ± 0.050	3.666 ± 0.015	16
69673	K0III CH-1 CN-0.5	20.877 ± 0.277	-0.050	-1.330 ± 0.027	-2.951 ± 0.050	–	1, 11, 17, 18, 19
72607	K4- III	10.300 ± 0.100	2.070	0.590 ± 0.027	–	-1.259 ± 0.070	1
74666	G8IV	2.744 ± 0.036	3.460	2.480 ± 0.027	1.260 ± 0.050	1.121 ± 0.031	1, 2, 3, 6
74793	K4III	2.336 ± 0.020	5.020	–	–	1.901 ± 0.051	12
75260	K4III	1.690 ± 0.031	5.720	–	–	2.721 ± 0.060	12
75458	K2III	3.596 ± 0.015	3.290	2.200 ± 0.027	–	0.701 ± 0.041	20
77070	K2III	4.828 ± 0.062	2.630	1.560 ± 0.027	0.197 ± 0.007	0.041 ± 0.051	1, 2
79882	G9.5IIIb Fe-0.5	2.961 ± 0.007	3.230	2.290 ± 0.027	–	0.961 ± 0.051	21
80331	G8III-IV	3.633 ± 0.066	2.730	1.890 ± 0.027	–	0.601 ± 0.031	1, 2
80816	G7IIIa Fe-0.5	3.492 ± 0.050	2.780	1.880 ± 0.027	0.690 ± 0.050	0.621 ± 0.041	1, 2
81833	G7III Fe-1	2.529 ± 0.050	3.480	2.580 ± 0.027	–	1.281 ± 0.031	1, 2, 3
82611	K2III	1.440 ± 0.004	5.990	–	–	2.811 ± 0.090	12
86182	K1III	1.515 ± 0.010	5.350	–	–	2.651 ± 0.070	12
87833	K5III	9.978 ± 0.180	2.240	0.630 ± 0.027	-1.160 ± 0.050	-1.319 ± 0.041	1, 11, 13, 17
90344	K1.5III Fe-1	2.120 ± 0.020	4.820	3.630 ± 0.027	–	1.931 ± 0.051	22
93194	A1III	0.753 ± 0.009	3.250	3.260 ± 0.027	3.195 ± 0.050	–	23
94376	G9III	3.268 ± 0.054	3.070	2.120 ± 0.027	–	0.741 ± 0.051	1, 2
96837	K0III	1.765 ± 0.012	4.390	3.410 ± 0.027	2.210 ± 0.050	2.071 ± 0.060	9
97938	G9.5IIIb	1.726 ± 0.008	4.710	3.630 ± 0.027	–	2.351 ± 0.090	24
98337	M0- III	6.821 ± 0.098	3.510	1.790 ± 0.027	-0.042 ± 0.050	-0.309 ± 0.041	1, 13, 25
99663	K5III	1.859 ± 0.003	5.810	–	–	2.311 ± 0.070	12
102488	K0III-IV	4.610 ± 0.050	2.480	1.450 ± 0.027	0.206 ± 0.050	0.101 ± 0.070	1
104732	G8+ IIIa Ba0.5	2.820 ± 0.030	3.210	2.270 ± 0.027	1.155 ± 0.050	1.051 ± 0.031	1
110538	G9IIIb Ca1	1.920 ± 0.020	4.420	3.400 ± 0.027	2.217 ± 0.050	1.961 ± 0.051	3
111944	K2.5III	2.731 ± 0.024	4.500	3.190 ± 0.027	1.600 ± 0.007	1.391 ± 0.070	12

Note. — **Angular Diameter References:** (1) Mozurkewich et al. (2003), (2) Nordgren et al. (2001), (3) Nordgren et al. (1999), (4) Mozurkewich et al. (1991), (5) Boyajian (2009), (6) van Belle (1999), (7) Richichi & Roccatagliata (2005), (8) White & Feigman (1987), (9) van Belle et al. (2009), (10) Shao et al. (1988), (11) di Benedetto (1993), (12) Baines et al. (2010), (13) Hutter et al. (1989), (14) Thévenin et al. (2005), (15) von Braun et al. (2014), (16) Crepp et al. (2012), (17) Dyck et al. (1996), (18) Quirrenbach et al. (1996), (19) di Benedetto & Foy (1986), (20) Baines et al. (2011), (21) Mazumdar et al. (2009), (22) Ligi et al. (2012), (23) Maestro et al. (2013), (24) Baines et al. (2009), (25) Wittkowski et al. (2001). **Color Magnitude References:** Neugebauer & Leighton (1969), Gezari et al. (1999), Carpenter (2001), Kidger & Martín-Luis (2003), Kimeswenger et al. (2004), Koen et al. (2010), and Mallama (2014); see Section 2 for more details.

fit of $\log \theta_{Q=0}$ and add polynomial terms in color, following the form of Equation 3. The fitting procedure uses a Levenberg-Markquardt least-squares algorithm provided by the *MPFIT* routine (Markwardt 2009). For each solution, we perform an F-test (Press et al. 1992) to determine whether the improvement to the relation by adding a polynomial

term is statistically significant. Once the functional form is obtained we run a Monte Carlo simulation by generating 10^4 simulated datasets, randomly choosing colors and diameters drawn from Gaussian probability distributions of each star’s true color and diameter. The means and standard deviations are given by the initial fit coefficients and their associated

uncertainties, respectively. This allows us to incorporate all measurement uncertainties into the relation.

4 ANALYSIS

For each color we construct independent fits of unevolved and evolved stars (Figure 1). Table 3 shows the number of stars, range of colors, and fit coefficients for each fit. These relations are only valid for the color ranges for which we have data. We then construct fits for each color using all stars, unevolved and evolved. The combined fits test that variations in surface gravity with stellar evolution will not affect the relations (as noted in Section 1). The derived relations with the combined sample have similar RMS errors to the separated fits, which is consistent with the result of Barnes & Evans (1976) that surface brightness is independent of luminosity class. The RMS in the residuals ranges from 0.017 to 0.03 dex, corresponding to the minimum expected uncertainties in $\log \theta_{LD}$ before uncertainties in magnitudes are considered. The $I_C - K$ relations have the smallest spread for all fits.

To estimate the uncertainties in limb-darkened diameters, we propagate uncertainties for assumed 0.03 errors in both magnitudes of a given color. The most precise relations for all stars are those for $V - H$ and $V - K$, which have estimated uncertainties of 1.8–2.9%. (The range is due to the dependence of the uncertainty on the color, which we have varied within the range of the sample.) The least precise results are in $V - I_C$, where the corresponding uncertainties could be as high as 6.5%.

Initially M dwarfs were included in our sample, to see if the derived relation would change drastically with their inclusion. The addition of dwarfs at $T < 3900$ K adds a statistically significant quadratic coefficient to our fits in the $V - I_C$ relation. Our temperature cut therefore provides a more precise relation for FGK stars in particular. In contrast the $V - I_C$ relation in giants has a marginally significant quadratic term, even excluding stars below 3900 K. On the other end of our temperature range, inclusion of the A dwarfs (and one A giant) did not significantly change the fits, and so we are less hesitant to include them here.

We also test whether the angular diameter relations have a statistically significant dependence on stellar metallicity. Metallicity has shown to be a factor in relations of stellar radii to color indices (Boyajian et al. 2012b), since changes in metallicity tend to affect bluer parts of the stellar spectra due to line blanketing (McNamara & Colton 1969). Such effects would propagate to stellar angular diameter relations, but in all colors considered in this paper the relations were insensitive to metallicity. This is consistent with the findings of Boyajian et al. (2014), which found metallicity in their angular diameter relations was strongest for the colors with the shortest wavelength bands ($B - V$, $g - r$), where the bluer colors would be affected more strongly by line blanketing.

4.1 Comparison with Previous Works

We directly compare our relations to those of Boyajian et al. (2014), and for $V - I_C$ to the relation in Table 3 of Kervella & Fouqué (2008), and the $V - K$ relation to Eq. (23) of Kervella et al. (2004b), as seen in Figure 1. All the

mentioned relations are valid for dwarfs and subgiants, and it should be noted that all extend through the M spectral type (not shown here). In $V - I_C$ the largest offset in angular diameter between the data and the Kervella & Fouqué (2008) prediction is 0.08 dex, and for $V - K$ the largest offset with respect to Kervella et al. (2004b) is 0.06 dex. We expect at least reasonable agreement with the results of Boyajian et al. (2014) and Kervella & Fouqué (2008) (see Figure 1) by construct, since we include the subset of angular diameters used in these works which meet our uncertainty constraint ($\leq 2\%$). Nevertheless, our sources differ from these works for I_C (Koen et al. 2010; Mallama 2014), H (Gezari et al. 1999), and K (Neugebauer & Leighton 1969; Kidger & Martín-Luis 2003; Kimeswenger et al. 2004) band photometry, as well as a larger sample within the FGK color range. Hence differences in the predicted angular diameters exist, particularly on the blue end of the $V - I_C$ relation, where both Kervella & Fouqué (2008) and Boyajian et al. (2014) use higher-order polynomial fits that underestimate the diameters of the bluest dwarfs, while fitting well for dwarfs well beyond the red end of our color range.

5 CONCLUSIONS

This work describes new relations linking stellar angular diameter to photometric colors. We use a dataset with roughly twice the precision in angular diameter measurements compared to previous papers. We use empirical evidence that predictions of angular diameters from color and magnitude are insensitive to luminosity class to construct, for the first time, a prediction of angular diameters at fixed magnitude for A–K stars across the stages of stellar evolution. We find that there is no dependence on stellar metallicity for the colors tested.

Further improvement to the relations will require additional angular diameter measurements to fill in parameter space for the earlier-type giants. Additionally, lack of demonstrably consistent I_C photometry for M stars of any luminosity class limits us from extending the red end of our relations. Transformations among systems are susceptible to differences in zero points, susceptibility of filters to red leaks, and correlated errors in the filter profiles (Mann & von Braun 2015). Nevertheless, for FGK stars the continuity in the relation between color and angular size is well-constrained by the regions of overlap of the spectral classes.

ACKNOWLEDGEMENTS

This work supported by a graduate fellowship from the Gruber Foundation. Additional gratitude to Anthony Mallama for providing converted Cousins I magnitudes for the dwarfs in our sample.

This research has made use of the NASA Exoplanet Archive, which is operated by the California Institute of Technology, under contract with the National Aeronautics and Space Administration under the Exoplanet Exploration Program.

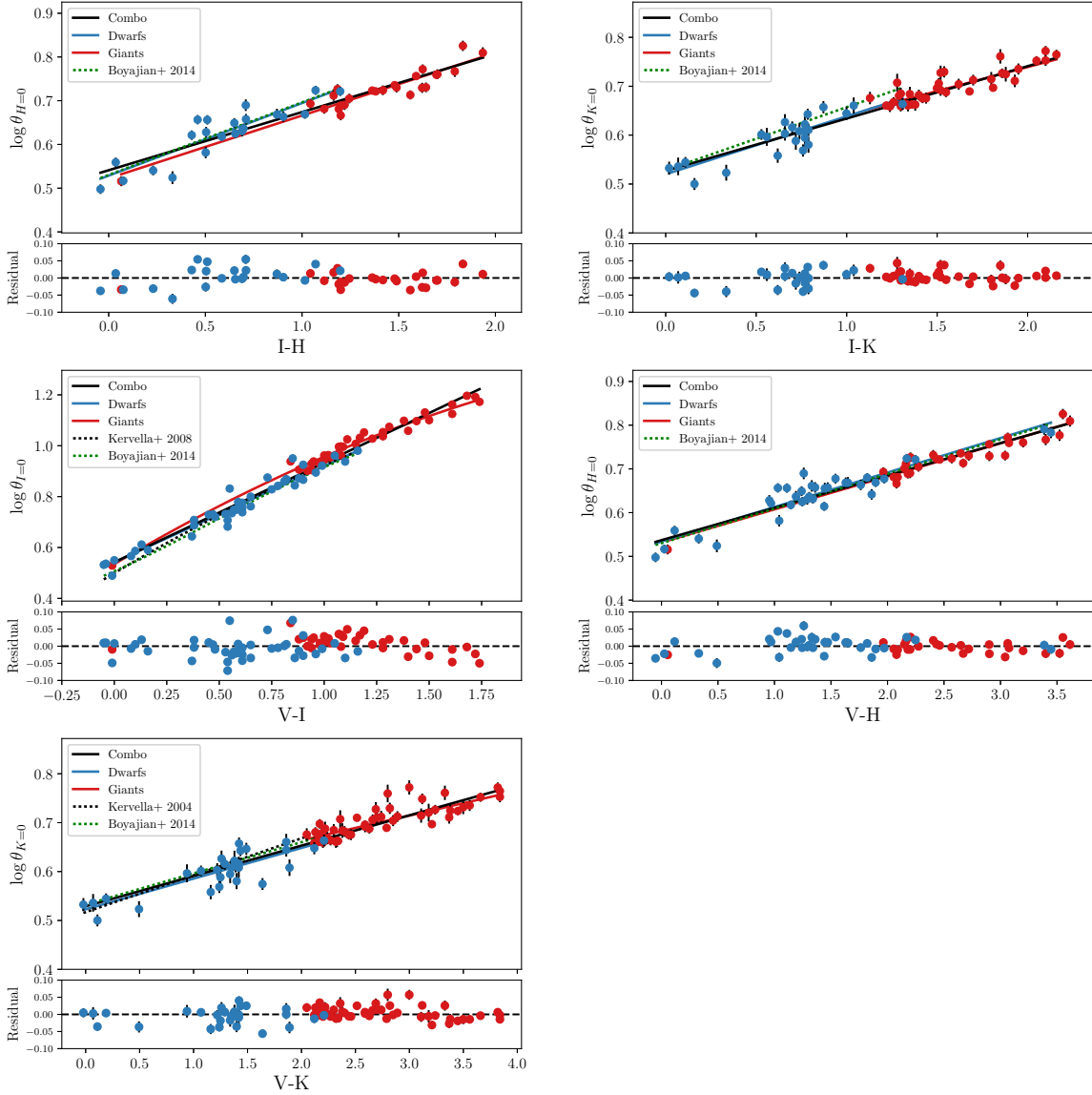


Figure 1. *Top panels:* Angular diameter-color relations for both dwarf/subgiants (blue line) and giants (red line), as well as a combined fit (black line). The functional form of the fits is described in Equation 3 with coefficients listed in Table 3. The data are introduced in Section 2 and catalogued in Tables 1–2. The fitting methodology is described in Section 4. All panels show previous relations from Boyajian et al. (2014). For $V - I_C$ we include the result for dwarfs from Kervella & Fouqué (2008), and for $V - K$ we include the result for dwarfs from Kervella et al. (2004b). *Bottom panels:* The residuals in dex are shown with respect to the combined relation.

REFERENCES

- Aufdenberg J. P., et al., 2006, *ApJ*, **645**, 664
- Baines E. K., McAlister H. A., ten Brummelaar T. A., Turner N. H., Sturmman J., Sturmman L., Goldfinger P. J., Ridgway S. T., 2008, preprint, 803 ([arXiv:0803.1411](https://arxiv.org/abs/0803.1411))
- Baines E. K., McAlister H. A., ten Brummelaar T. A., Sturmman J., Sturmman L., Turner N. H., Ridgway S. T., 2009, *ApJ*, **701**, 154
- Baines E. K., et al., 2010, *ApJ*, **710**, 1365
- Baines E. K., et al., 2011, *ApJ*, **731**, 132
- Barnes T. G., Evans D. S., 1976, *MNRAS*, **174**, 489
- Boyajian T. S., 2009, PhD thesis, Georgia State University
- Boyajian T. S., et al., 2008, *ApJ*, **683**, 424
- Boyajian T. S., et al., 2012a, *ApJ*, **746**, 101
- Boyajian T. S., et al., 2012b, *ApJ*, **757**, 112
- Boyajian T. S., et al., 2013, *ApJ*, **771**, 40
- Boyajian T. S., van Belle G., von Braun K., 2014, *AJ*, **147**, 47
- Boyajian T., et al., 2015, *MNRAS*, **447**, 846
- Calchi Novati S., et al., 2010, *ApJ*, **717**, 987
- Carpenter J. M., 2001, *AJ*, **121**, 2851
- Chiavassa A., Bigot L., Kervella P., Matter A., Lopez B., Collet R., Magic Z., Asplund M., 2012, *A&A*, **540**, A5
- Ciardi D. R., van Belle G. T., Akeson R. L., Thompson R. R., Lada E. A., Howell S. B., 2001, *ApJ*, **559**, 1147
- Crepp J. R., et al., 2012, *ApJ*, **751**, 97
- Cutri R. M., et al., 2003, The 2MASS All Sky Catalog of Point Sources. Pasadena: IPAC
- Davis J., Tango W. J., 1986, *Nature*, **323**, 234
- Davis J., Ireland M. J., North J. R., Robertson J. G., Tango W. J., Tuthill P. G., 2011, *Publications of the Astronomical Society of Australia*, **28**, 58

Table 3. Angular Diameter - Color Relations

Color	N	Range	c_0	c_1	c_2	RMS (dex)	Pred. Frac. Uncertainty
All Stars							
$I_C - H$	47	-0.042–1.935	0.541±0.004	0.133±0.003	—	0.025	0.021–0.031
$I_C - K$	60	0.019–2.159	0.528±0.005	0.108±0.003	—	0.020	0.021–0.031
$V - I_C$	83	-0.050–1.740	0.542±0.006	0.391±0.006	—	0.028	0.043–0.065
$V - H$	63	-0.052–3.615	0.538±0.004	0.074±0.002	—	0.020	0.018–0.029
$V - K$	78	-0.021–3.839	0.529±0.004	0.062±0.002	—	0.021	0.018–0.029
Dwarfs and Subgiants							
$I_C - H$	22	-0.042–1.198	0.529±0.007	0.166±0.010	—	0.031	0.026–0.049
$I_C - K$	24	0.019–1.309	0.520±0.007	0.118±0.010	—	0.023	0.024–0.047
$V - I_C$	45	-0.050–1.160	0.542±0.007	0.378±0.011	—	0.029	0.043–0.070
$V - H$	35	-0.052–3.447	0.534±0.005	0.079±0.003	—	0.023	0.020–0.036
$V - K$	29	-0.021–2.209	0.523±0.006	0.063±0.005	—	0.024	0.022–0.038
Giants							
$I_C - H$	25	0.065–1.935	0.523±0.011	0.144±0.007	—	0.020	0.033–0.054
$I_C - K$	36	1.129–2.159	0.543±0.011	0.098±0.007	—	0.016	0.040–0.053
$V - I_C$	38	-0.010–1.740	0.535±0.027	0.490±0.046	-0.068±0.019	0.026	0.080–0.241
$V - H$	28	0.055–3.615	0.532±0.009	0.076±0.003	—	0.016	0.026–0.041
$V - K$	49	2.049–3.839	0.562±0.009	0.051±0.003	—	0.019	0.031–0.040

Note. — Numerical values for the relations in Figure 1. The color index, number of stars per index, range of color, and fit coefficients for Equation 3 (which takes the form $\log \theta_{Q=0} = \sum_{n=0}^N c_n (P - Q)^n$) are shown. For each relation we have calculated both the RMS of the relation and the range of propagated fractional uncertainties for each zero-magnitude angular diameter, assuming 0.03 mag errors in each band.

- Demory B., et al., 2009, *A&A*, **505**, 205
- Di Benedetto G. P., 2005, *MNRAS*, **357**, 174
- Di Folco E., Thévenin F., Kervella P., Domiciano de Souza A., Coudé du Foresto V., Ségransan D., Morel P., 2004, *A&A*, **426**, 601
- Dyck H. M., Benson J. A., van Belle G. T., Ridgway S. T., 1996, *AJ*, **111**, 1705
- Freeman P., Doe S., Siemiginowska A., 2001, in Starck J.-L., Murtagh F. D., eds, Proc. SPIE Vol. 4477, Astronomical Data Analysis. pp 76–87 ([arXiv:astro-ph/0108426](https://arxiv.org/abs/astro-ph/0108426)), doi:10.1117/12.447161
- Fukui A., et al., 2015, *ApJ*, **809**, 74
- Gezari D. Y., Pitts P. S., Schmitz M., 1999, VizieR Online Data Catalog, **2225**, 0
- Hanbury Brown R. H., Davis J., Lake R. J. W., Thompson R. J., 1974, *MNRAS*, **167**, 475
- Hunter J. D., 2007, *Computing in Science Engineering*, **9**, 90
- Hutter D. J., et al., 1989, *ApJ*, **340**, 1103
- Iyengar K. V. K., Strafella F., Lorenzetti D., Cosmovici C. B., 1982, *Journal of Astrophysics and Astronomy*, **3**, 451
- Kervella P., Fouqué P., 2008, *A&A*, **491**, 855
- Kervella P., Thévenin F., Morel P., Bordé P., Di Folco E., 2003, *A&A*, **408**, 681
- Kervella P., et al., 2004a, in Dupree A. K., Benz A. O., eds, IAU Symposium Vol. 219, Stars as Suns : Activity, Evolution and Planets. p. 80
- Kervella P., Thévenin F., Di Folco E., Ségransan D., 2004b, *A&A*, **426**, 297
- Kidger M. R., Martín-Luis F., 2003, *AJ*, **125**, 3311
- Kimeswenger S., et al., 2004, *A&A*, **413**, 1037
- Koen C., Kilkeny D., van Wyk F., Marang F., 2010, *MNRAS*, **403**, 1949
- Koornneef J., 1983, *A&AS*, **51**, 489
- Ligi R., et al., 2012, *A&A*, **545**, A5
- Maestro V., et al., 2013, *MNRAS*, **434**, 1321
- Mallama A., 2014, Journal of the American Association of Variable Star Observers (JAAVSO), **42**, 443
- Mann A. W., von Braun K., 2015, *PASP*, **127**, 102
- Markwardt C. B., 2009, in D. A. Bohlender, D. Durand, & P. Dowler ed., Astronomical Society of the Pacific Conference Series Vol. 411, Astronomical Data Analysis Software and Systems XVIII. pp 251–+ ([arXiv:0902.2850](https://arxiv.org/abs/0902.2850))
- Mazumdar A., et al., 2009, *A&A*, **503**, 521
- McKinney W., 2010, in van der Walt S., Millman J., eds, Proceedings of the 9th Python in Science Conference. pp 51 – 56
- McNamara D. H., Colton D. J., 1969, *PASP*, **81**, 826
- Monnier J. D., et al., 2012, *ApJ*, **761**, L3
- Mozurkewich D., et al., 1991, *AJ*, **101**, 2207
- Mozurkewich D., et al., 2003, *AJ*, **126**, 2502
- Neugebauer G., Leighton R. B., 1969, Two-micron sky survey. A preliminary catalogue. NASA SP, Washington: NASA, 1969
- Nordgren T. E., et al., 1999, *AJ*, **118**, 3032
- Nordgren T. E., Sudol J. J., Mozurkewich D., 2001, *AJ*, **122**, 2707
- Press W. H., Teukolsky S. A., Vetterling W. T., Flannery B. P., 1992, Numerical recipes in C. The art of scientific computing. Cambridge: University Press, |c1992, 2nd ed.
- Quirrenbach A., Mozurkewich D., Buscher D. F., Hummel C. A., Armstrong J. T., 1996, *A&A*, **312**, 160
- Richichi A., Roccatagliata V., 2005, *A&A*, **433**, 305
- Shao M., et al., 1988, *ApJ*, **327**, 905
- Thévenin F., Kervella P., Pichon B., Morel P., di Folco E., Lebreton Y., 2005, *A&A*, **436**, 253
- Wesselink A. J., 1969, *MNRAS*, **144**, 297
- White N. M., Feierman B. H., 1987, *AJ*, **94**, 751
- Wittkowski M., Hummel C. A., Johnston K. J., Mozurkewich D., Hajian A. R., White N. M., 2001, *A&A*, **377**, 981
- di Benedetto G. P., 1993, *A&A*, **270**, 315
- di Benedetto G. P., Foy R., 1986, *A&A*, **166**, 204
- di Folco E., et al., 2007, *A&A*, **475**, 243
- van Belle G. T., 1999, *PASP*, **111**, 1515
- van Belle G. T., Creech-Eakman M. J., Hart A., 2009, *MNRAS*, **394**, 1925
- van Leeuwen F., 2007, *A&A*, **474**, 653
- van der Walt S., Colbert S. C., Varoquaux G., 2011, *Computing in Science Engineering*, **13**, 22

von Braun K., et al., 2011, [ApJ](#), 740, 49

von Braun K., et al., 2014, [MNRAS](#), 438, 2413

This paper has been typeset from a $\text{T}_{\text{E}}\text{X}/\text{L}^{\text{A}}\text{T}_{\text{E}}\text{X}$ file prepared by the author.